ARTICLE NO. 78-569R

High Pointing Accuracy with a Momentum Bias Attitude Control System

K.L. Lebsock*
Hughes Aircraft Co., El Segundo, Calif.

A new design procedure for momentum bias attitude control systems is presented and applied to the design of the roll/yaw control loop for a two-axis momentum storage system. This procedure generates a set of system parameters that results in a prescribed yaw and roll pointing accuracy for a given disturbance torque environment. A breadboard model of the control system has been developed, and hybrid tests of the hardware operating in conjunction with an analog computer have been conducted. Test results demonstrate the high pointing accuracy of the two-axis momentum storage system.

Introduction

THE continuing evolution of communications satellite system requirements has been toward long-life high-power geostationary spacecraft employing multiple narrowbeam antennas. In order to meet the reliability and pointing requirements of future communications satellites, it will be necessary to re-examine the control system configurations and strategy used on existing satellites. For example, the most common three-axis systems used to date have been momentum bias systems using two-axis sensing (e.g., a horizon sensor providing pitch and roll information) and one axis (pitch) of momentum storage.[1] Systems of this type such as Symphonie, FLTSatcom, and Intelsat V have pointing accuracies in the range 0.2-1.0 deg. A significant improvement in roll pointing accuracy can be achieved by introducing a second axis of momentum storage capability, either by means of a yaw reaction wheel or by gimbaling the pitch bias wheel about the roll axis. The higher roll pointing accuracy is due primarily to the filtering of sensor noise and the rapid damping of transients provided by the yaw axis momentum control loop. In addition, the pitch momentum bias required for a prescribed yaw pointing accuracy is generally smaller for a two-axis momentum storage system than for a one-axis system.

This paper describes the development and testing of a high-performance momentum bias system that uses a yaw reaction wheel. This system has been selected on the basis of a tradeoff study focusing primarily on the requirements of attitude control accuracy of 0.05 deg in pitch and roll (excluding sensor biases) and 0.15 deg in yaw and 7-yr design life with no possible single-point failures.

The on-orbit attitude control system consists of a small variable speed wheel aligned with the yaw axis, two larger variable speed momentum wheels canted off slightly from the pitch axis, redundant horizon sensors to measure pitch and roll errors, and an assembly of hydrazine thrusters to provide momentum desaturation torques and stationkeeping thrust. The pitch attitude is controlled by varying the pitch momentum wheel speed ±5% about a nominal bias value. Roll attitude is controlled and roll/yaw nutation is damped by varying the angular momentum along the yaw axis. The momentum bias of the pitch wheel provides yaw restraint and, together with the orbital kinematics, transfers yaw errors into roll for correction by the yaw axis momentum control system. Excessive accumulation of angular momentum on either wheel due to secular environmental torques is prevented by firing a short pulse from a hydrazine thruster. The pitch axis momentum bias and the roll/yaw desaturation deadband are determined by pointing accuracy requirements and the disturbance torques acting on the spacecraft.

Presented as Paper 78-569 at the AIAA 7th Communications Satellite Systems Conference, San Diego, Calif., April 24-27, 1978; submitted July 11, 1978; revision received Nov. 5, 1979.

Index categories: Spacecraft Dynamics and Control; Spacecraft Systems.

*Senior Staff Engineer, Space Flight Mechanics Department, Systems Analysis and Design Laboratory.

Disturbance Torque Model

The satellite control axes (body frame X, Y, Z) are central principal axes of the satellite and nominally aligned with the orbital axes (orbit frame X_0, Y_0, Z_0), as shown in Fig. 1. The orbit frame rotates in inertial space at orbit rate ω_0 about the $-Y_0$-axis which is normal to the orbit plane. The X_0-axis is in the direction of the satellite's velocity, and the Z_0-axis is directed along the radius vector from the spacecraft to the center of the Earth. The orientation of the body frame is related to the orbital frame by the Euler angles ϕ (roll), θ (pitch), and ψ (yaw). The angular momentum vector of the momentum/reaction wheels is nominally directed along the negative Y-axis with a nominal bias value of H_N for a momentum bias system.

The external torques T_X and T_Z consist of control moments (M_{CX} and M_{CZ}) and environmental disturbance torques. For a synchronous communications satellite, the dominant environmental torques are usually the result of solar radiation pressure. Assuming that the attitude excursions are small, the solar torque becomes a function of orbital position and can be represented by a Fourier series. The coefficients of the series expansion of the environmental torque vary slowly over the course of a year and can be considered nearly constant over the course of several orbits. For preliminary design purposes it is usually sufficient to truncate the series after the first harmonic, unless such effects as shadowing or variations in surface reflective properties produce large magnitudes of the higher-order terms. Considering only the first harmonic terms of the environmental torque, the total external torque acting on the spacecraft in the orbit plane can be approximated by

$$T_X = M_{CX} + M_{BX} + M_I \sin(\omega_0 t + \gamma) \quad (1)$$

$$T_Z = M_{CZ} + M_{BZ} + M_I \cos(\omega_0 t + \gamma) \quad (2)$$

The terms M_{CX} and M_{CZ} are the roll and yaw components of the control torques (e.g., thruster torques) and can be

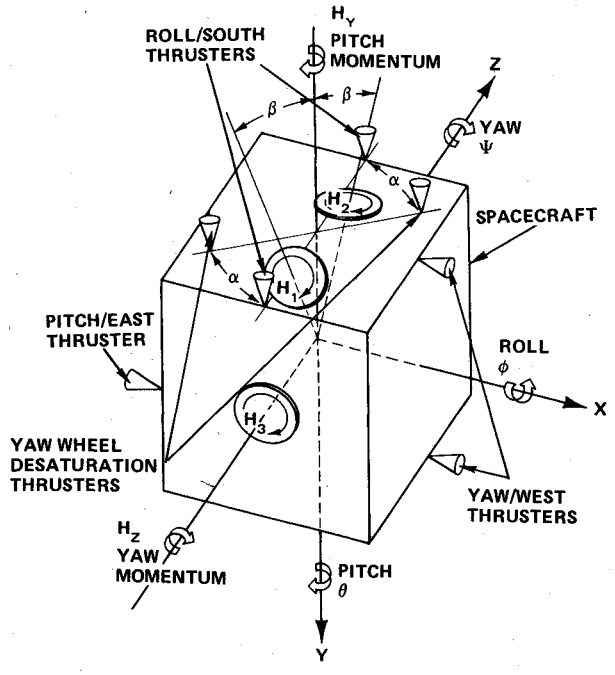

Fig. 1 Spacecraft coordinates and orientation of control system components.

functions of the control system states and time. The terms M_{BX} and M_{BZ} are body-fixed constant roll and yaw torques and are cyclic in an inertial reference frame. The quantity M_I is the orbit plane component of an inertially fixed torque and cycles between roll and yaw in the body-fixed reference frame. In practice, the value of M_I should be determined by finding the average value of the roll/yaw plane torques resolved in an inertial frame, rather than simply truncating the Fourier series of these torques resolved in the body frame.

Desaturation Requirements

The inertially constant component of the environmental torque M_I causes a secular increase in angular momentum which must be removed by control torques provided by a desaturation system. For a desaturation system using body-fixed offset roll/yaw thrusters, the control torques for desaturation are

$$M_{CX} = M_D \cos\alpha \tag{3}$$

$$M_{CZ} = -M_D \sin\alpha \tag{4}$$

The efficiency of the desaturation system can be defined as the ratio of the daily secular momentum increase due to environmental torques to the angular impulse provided by the desaturation thrusters; that is,

$$\eta \equiv \frac{\int_0^{2\pi/\omega_0} M_I \mathrm{d}t}{\sum_{j=1}^{n} (M_D \Delta t)_j} \tag{5}$$

where n is the number of roll/yaw firings per day and $(M_D \Delta t)_j$ is the angular impulse of the jth roll/yaw thruster firing. A reasonable design goal is for the desaturation efficiencies to be greater than 0.85.

In all momentum bias systems there is a continuous interchange of stored angular momentum between the roll and yaw axes due to the orbital kinematics. This momentum can be stored either as an attitude displacement (roll or yaw error) or in a wheel (e.g., yaw reaction wheel). The magnitude of the stored roll/yaw momentum increases secularly due to the inertially fixed torque M_I until control torques M_{CX} and/or M_{CZ} are applied to desaturate the system.

The desaturation control torques are commanded in response to some measure of the stored roll/yaw momentum. The total angular momentum along the X_0-axis is unobservable for a system without a yaw sensor. Thus the desaturation system is usually driven by an approximate measure of the angular momentum along the Z_0-axis (yaw momentum) formed from tachometer and horizon sensor signals. In a one-axis (pitch) momentum storage system the yaw momentum signal is $H_{Z0} \simeq -H_N \phi$. In a two-axis momentum storage system, such as presented in this paper, the yaw momentum signal is $H_{Z0} \simeq H_Z - H_N \phi$ where H_Z is the Z-axis component of the angular momentum of all the wheels. In most systems the desaturation torques are applied about an axis fixed in the roll/yaw plane of the satellite whenever the yaw momentum signal exceeds a deadband H_{DB}.

Roll/Yaw Limit Cycle

Although the roll/yaw desaturation system may also control roll attitude as in a one-axis momentum storage system, the emphasis of the following discussion is on yaw control; consequently, nutational dynamics are relatively unimportant.[2] During normal operation, the desaturation system functions as a yaw attitude control loop in a limit cycle at orbit rate. In general, a limit cycle is a trajectory contained within a discrete, closed region of space about an equilibrium point. The equilibrium point of the roll/yaw limit cycle is established by the momentum offsets required to balance the constant roll and yaw body-fixed environmental torques acting on the spacecraft. The limit cycle consists of a spiral divergence of the roll/yaw momentum away from this point under the influence of the inertially fixed torque until one edge of the deadband is encountered. Control torques are then applied to translate the state of the system along the edge of the deadband. The control torques terminate whenever the orbital kinematics move the state of the system away from the edge and back into the interior of the deadband. The subsequent motion is then dominated by the spiral divergence away from the equilibrium point until an edge of the deadband is encountered again.

Precise modeling of the control torques is relatively unimportant in determining an outer bound for the roll/yaw limit cycle provided that their application at the edge of the deadband stops the spiral divergence without creating excessive nutation transients. Using this assumption, the outer bound of the limit cycle in the roll/yaw momentum plane is made up of segments of the deadband edge and spiral arcs in the interior of the deadband. Ignoring nutational dynamics, the boundary conditions of the roll/yaw momentum trajectories require that the spiral arc segments depart tangentially from the deadband. Typical limit cycle momentum trajectories are shown in Figs. 2a and 2b for two different levels of roll bias torque. The common two-sided limit cycle as shown in Fig. 2a is characteristic of low values of roll bias torque M_{BX} and/or high values of inertial torque M_I, compared to the product $\omega_0 H_{DB}$. The one-sided limit cycle, as shown in Fig. 2b, is characteristic of high values of M_{BX} and/or low values of M_I. Since the efficiency of the limit cycle control torques drops off rapidly for spiral poles outside the deadband, the only limit cycles considered here are those for which $M_{BX} \leq \omega_0 H_{DB}$. This decrease in efficiency is the result of control torque, rather than just gyroscopic torque, being used to balance out the roll bias torque.

Normalized Design Curves

The equations describing the outer bounds of the momentum trajectories of the roll/yaw limit cycle have been evaluated on a digital computer for a wide range of system parameters and orbital environments. The results are most conveniently presented in normalized form, as shown in Fig. 3, where the normalized yaw angle L, and disturbance torques

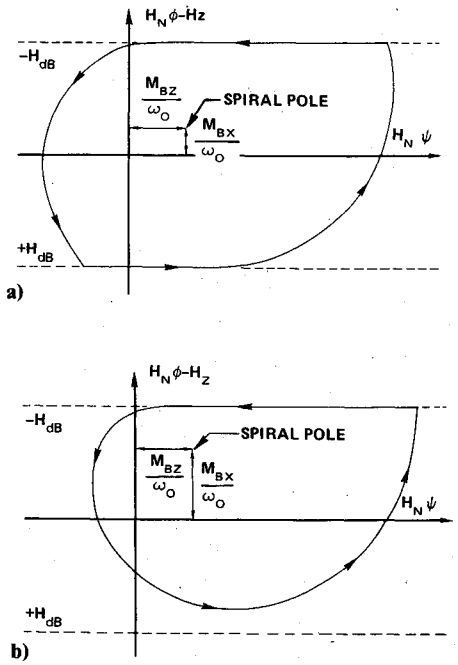

Fig. 2 Roll/yaw limit cycle: a) two-sided, b) one-sided.

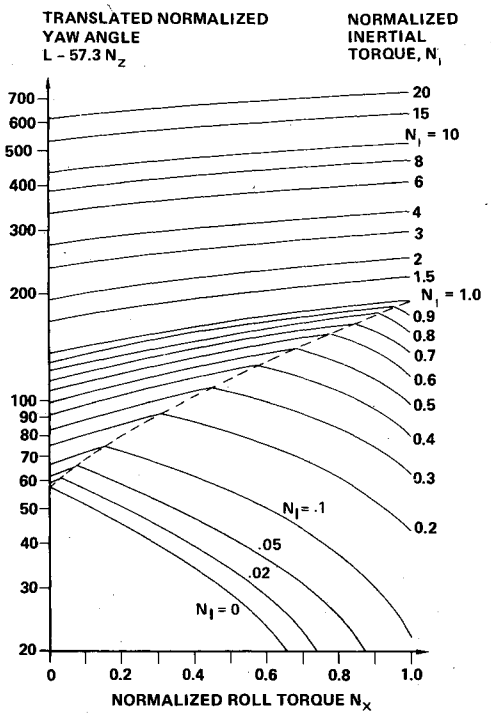

Fig. 3 Normalized momentum bias limit cycle design curves.

N_X, N_Z, and N_I are defined as

$$L = H_N \psi_{\max} / H_{DB} \tag{6}$$

$$N_X \equiv M_{BX} / \omega_0 H_{DB} \tag{7}$$

$$N_Z \equiv M_{BZ} / \omega_0 H_{DB} \tag{8}$$

$$N_I \equiv M_I / \omega_0 H_{DB} \tag{9}$$

The effect of the normalized yaw torque is to shift the momentum trajectories parallel to the edge of the deadband without altering their shape. Hence, the contribution to the maximum yaw angle caused by the constant yaw torque can

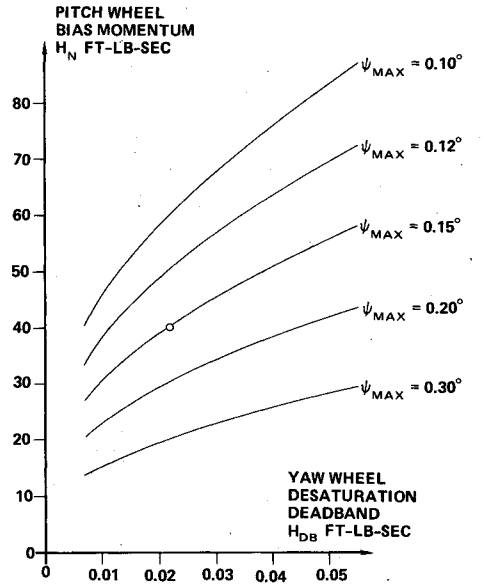

Fig. 4 Design curves for breadboard attitude control system.

be found from the equation

$$\psi_{SE} = M_{BZ} / \omega_0 H_N \tag{10}$$

The ordinate of the normalized graph is based upon the maximum yaw angle being expressed in degrees rather than radians, and subtracting the yaw angle contribution due to the yaw torque. The graph is thus a plot of translated normalized yaw angle ($L - 57.3\,N_Z$) vs the normalized roll torque (N_X) for different values of normalized roll/yaw inertial torque (N_I). Note that the normalized roll torque does not exceed unity in order to keep the spiral pole inside the deadband. The figure is divided into two regions by the dashed line: the region above and to the left of the dashed line corresponds to two-sided limit cycles, whereas the region below and to the right is associated with one-sided limit cycles.

Design Criteria Application

As an example of the use of the normalized curves, consider the design of a two-wheel control system with the following environment and attitude pointing requirements:

$$\omega_0 = 7.292 \times 10^{-5} \text{rad/s}$$

$$M_{BX} = 0.5 \times 10^{-6} \text{ft-lb}$$

$$M_{BZ} = 1.0 \times 10^{-6} \text{ft-lb}$$

$$M_I = 4.0 \times 10^{-6} \text{ft-lb}$$

$$\psi_{\max} = 0.15 \text{ deg}$$

$$\phi_{\max} = 0.05 \text{ deg}$$

Table 1 Breadboard attitude control system design parameters

N_I	H_{DB}, ft-lb-s	N_X	$L - 57.3N_Z$	$H_N\psi_{\max}$, ft-lb-s-deg
1.0	0.054855	0.1250	144	8.71
1.5	0.036570	0.1875	179	7.35
2.0	0.027427	0.2500	210	6.54
3.0	0.018285	0.3750	263	5.59
4.0	0.013714	0.5000	310	5.03
6.0	0.009143	0.7500	393	4.83
8.0	0.006857	1.0000	468	4.00

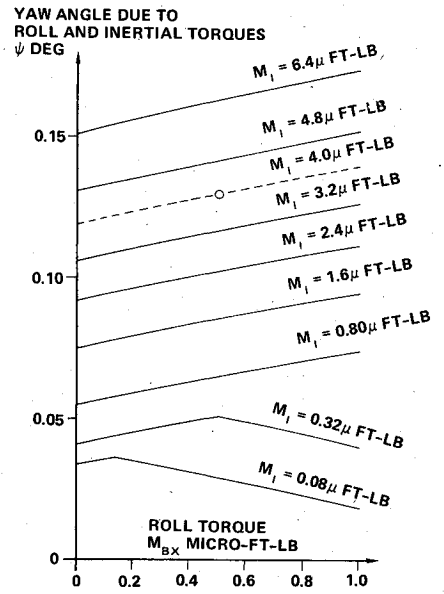

Fig. 5 Environmental torque sensitivity curves for breadboard attitude control system.

The normalized curves are used to construct a table of related quantities (see Table 1) which can be plotted as the conventional design curves (see Fig. 4). To construct the table, values of the desaturation deadband are calculated from Eq. (9) corresponding to several of the different levels of normalized inertial torque appearing on the graph. The normalized roll torque associated with this deadband is then found from Eq. (7). Next, the graph is used to find the value of $(L-57.3\ N_Z)$ corresponding to the values of N_I and N_X used above. From this quantity the product $H_N\psi_{\max}$ can be calculated from Eqs. (6) and (8). This product is then divided by five different levels of maximum yaw offset and the resulting value of bias momentum plotted against deadband size.

The nominal design point $H_N = 40$ ft-lb-s and $H_{DB} = 0.22$ ft-lb-s is chosen from the $\psi_{\max} = 0.15$ deg curve on the bases of wheel size availability and constraints on the deadband size. The deadband must be large enough so that a single desaturation impulse cannot drive the system into the opposite edge of the deadband. This can be expressed as

$$2H_{DB} \cong \Delta H_1 + \Delta H_2 + \Delta H_{DYN} \tag{11}$$

where ΔH_1 is the uncertainty of measurement of yaw axis momentum on the deadband edge initiating the pulse, ΔH_2 is the measurement uncertainty of the opposite deadband edge, and ΔH_{DYN} is the maximum change in the actual yaw axis momentum due to the nutational motion produced by the desaturation pulse. The dynamic change in momentum due to a thruster impulse $\Delta H = 0.02$ ft-lb-s applied at an angle of $\alpha = 45$ deg to the edge of the deadband is

$$\Delta H_{DYN} = \Delta H(1 + \sin\alpha) = 0.034 \text{ ft-lb-s} \tag{12}$$

Thus, if the desaturation signal is filtered so that $\Delta H_1 + \Delta H_2 \simeq H_1 + \Delta H_2 \leq 0.010$ ft-lb-s, then Eq. (11) indicates that a deadband of $H_{DB} = 0.022$ ft-lb-s is the minimum acceptable and establishes the design point given above. The selection of the thruster offset angle α is not critical for a two-axis momentum storage system and is often[3,4] set equal to 45 deg.

The normalized curves can also be used for sensitivity studies once a nominal design point is selected. For example, in the design just given, the nominal values of the constant roll and inertial torques together contribute 0.13 deg and the nominal yaw torque contributes 0.02 deg to the maximum yaw error of 0.15 deg. The actual values of these torque components for a synchronous spacecraft will vary throughout the year and result in different yaw errors. The contribution to the total yaw error due to the yaw torque component can be found directly from Eq. (10). The contribution due to the roll and inertial components can be found from the normalized graph using a process similar to that described previously for generating the design curves. The yaw angle sensitivity to roll and inertial torques is shown in Fig. 5. The dashed curve passing through the nominal design point is an interpolated curve, whereas all the other curves are taken from lines of constant N_I in the normalized graph. The change in slope of the lowest two curves in Fig. 5 is due to the transition from a two- to a one-sided limit cycle. The sensitivity curves and Eq. (10) reveal the relative importance of the various torque components to the yaw pointing accuracy. This permits the systems engineer to concentrate on methods of torque balancing, such as spacecraft configuration control or the addition of magnetic coils, that will result in the greatest improvement in performance.

System Selection

The evolution of the single-axis momentum storage configuration into a two-axis configuration in order to achieve a high accuracy momentum bias system proceeds as follows. The information presented in Fig. 4 can be used to select the roll readband for a single-axis momentum storage system[2,5]

$$\phi_{DB} = 57.3\ H_{DB}/H_N \tag{13}$$

Using the same pointing requirements and minimum thruster impluse bit as in the preceding section, Eq. (13) in conjunction with the minimum impulse bit equations of Ref. 2 results in a design with $H_{DB} = 0.046$ ft-lb-s, $\alpha = 12$ deg, and $H_N = 53$ ft-lb-s. In this case, the momentum deadband H_{DB} has to be increased to account for larger dynamic excursions due to nutation. This requires a larger value of pitch axis bias momentum H_N to achieve the same yaw pointing accuracy as a two-axis momentum storage system. Rather than accept the weight penalty of using larger redundant pitch wheels, it becomes more effective to add a single yaw wheel.

The resulting three-wheel system shown in Fig. 1 provides momentum bias about the pitch axis, momentum storage in both the pitch and yaw axes, and is completely redundant. In addition, due to the cant angle of the pitch wheels, the yaw wheel operates at a nominal bias value. Consequently, control system errors due to stiction and tachometer measurement difficulties associated with operating a reaction wheel about zero speed are eliminated. The cant angle β is chosen so that the yaw component of the angular momentum of a single canted pitch wheel operating at nominal speed is at the midpoint of the operating range of the yaw reaction wheel. The minimum speed of the yaw wheel operating range is set by the desired level of tachometer resolution and the maximum speed is set by the total yaw axis momentum storage required between desaturation pulses.

A further advantage of the two-axis momentum storage configuration over the single-axis momentum storage configuration is that the roll and yaw pointing accuracies can be set independently. In the single-axis configuration, the deadband sets both the roll and yaw pointing accuracies, whereas in the two-axis configuration, the roll accuracy is determined by the yaw wheel control loop response to desaturation pulses. In fact, the roll pointing accuracy can be set to approximately one-half of the peak-to-peak amplitude of the roll transient caused by a single desaturation pulse. This is accomplished by commanding a yaw wheel speed bias prior to firing a desaturation pulse and then removing the command once the pulse is fired. This method results in a roll bias error being introduced before the firing and then a transient that reaches a peak value of opposite sign and approximately equal magnitude after the firing. The mechanization of this

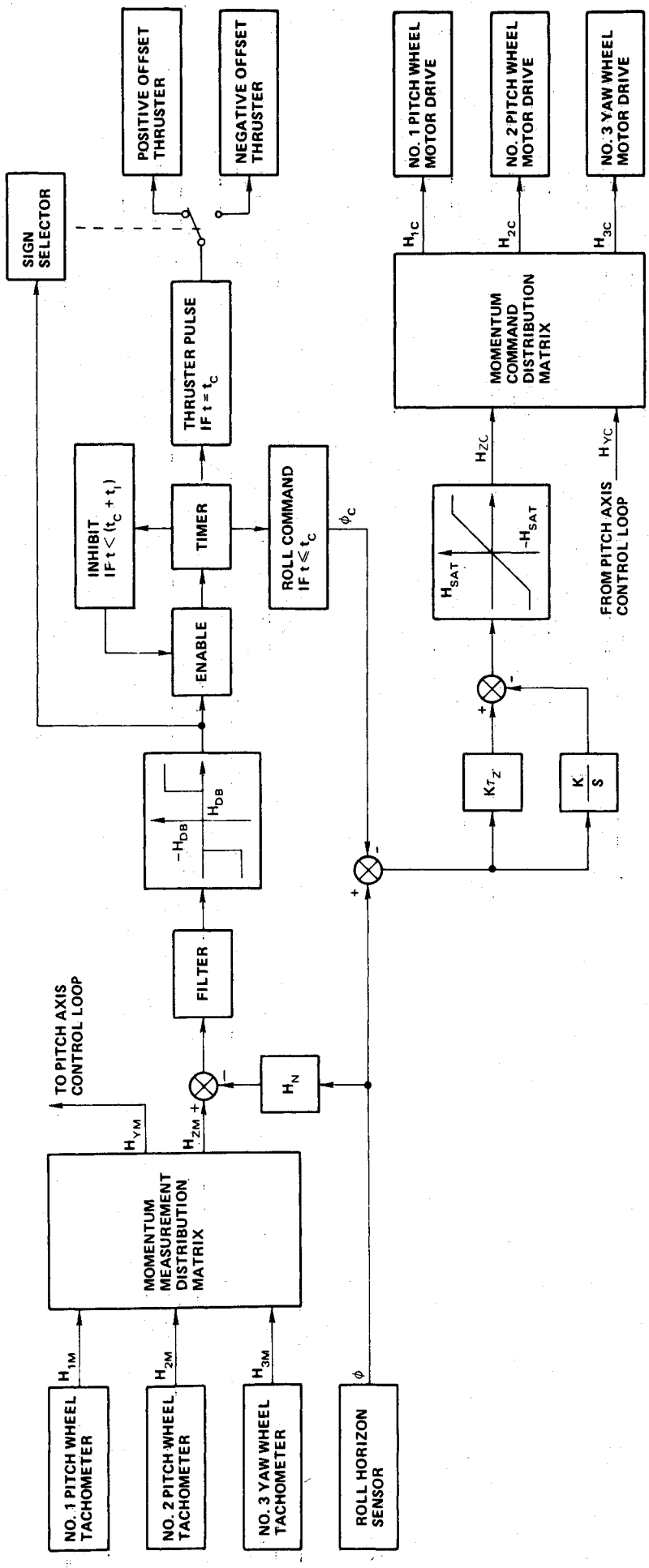

Fig. 6 Roll/yaw attitude control system block diagram.

scheme is shown in Fig. 6 where the roll command signal is:

$$\phi_C = 57.3\, M_D \Delta t / H_N \tag{14}$$

where Δt is the pulse duration of the desaturation firing.

Roll/Yaw Control Loops

The roll/yaw control system consists of two distinct loops: 1) the yaw axis momentum control loop and 2) the yaw axis momentum desaturation loop. In practice, additional roll and yaw gas loops are needed for large angle acquisition and orbit adjust maneuvers, but such control loops are beyond the scope of this paper.

During normal on-orbit operation the yaw axis momentum control loop provides vernier roll control and nutation damping. This is accomplished by varying the yaw angular momentum in response to the roll attitude error measured by the horizon sensor. Internal tachometer loops are included in the motor drives for each wheel to provide momentum command implementation for both the pitch and yaw momentum control loops. The time constants of these tachometer loops are chosen to supply a compensation pole for the yaw axis momentum control loop. The electronic compensation for this loop is of the nonminimum phase zero form[3] (integral minus proportional) although other forms[4,6] have been considered. This form of compensation was chosen because of its insensitivity to horizon sensor noise and its rapid damping of transients. The loop parameters were selected in accordance with the suggestions of Ref. 1 and 3. This loop directly controls the roll attitude and rate errors. It also provides rapid nutational damping since the yaw rate is gyroscopically coupled to the roll axis motion by the bias momentum along the pitch axis. Indirect yaw attitude control is achieved by the kinematical coupling of yaw into roll that results from the orbit rate rotation of the control reference frame about the orbit normal.

The yaw wheel desaturation loop provides momentum dumping of the secular momentum accumulated in the roll/yaw plane during normal on-orbit operation. This is accomplished by firing roll/yaw thruster pulses in response to the Z_0-axis component of angular momentum. An approximate measurement of this momentum is formed from a filtered combination of the roll horizon sensor error and the reaction wheel tachometer signals. The roll error signal is near null in configurations that do not have to track a time varying roll pointing command and, consequently, could be eliminated from the momentum measurement in order to further desensitize the system to sensor noise. The processing of the Z_0-axis momentum signal is performed by a deadband circuit, a pulse timer, and an inhibit circuit. This loop serves as an outer control loop for the roll axis and performs the same basic functions as the offset thruster loop on a single-wheel momentum bias system[2,5] operating in the limit cycle mode.

Table 2 Roll/yaw control loop parameters

I_x	Roll moment of inertia (MOI)	400 slug-ft^2
I_y	Pitch MOI	100 slug-ft^2
I_z	Yaw MOI	400 slug-ft^2
ω_0	Orbit rate	7.29×10^{-5} rad/s
H_N	Pitch bias momentum	40 ft-lb-s
β	Pitch wheel cant angle	−0.891 deg
τ_m	Tach loop time constant	14.29 s
τ_z	Zero time constant	53.64 s
K	Proportional gain	0.3500 ft-lb/rad
H_{sat}	Wheel saturation	0.893 ft-lb-s
I_w	Yaw wheel MOI	0.0108 slug-ft^2
H_{DB}	Deadband	0.022 ft-lb-s
Δt	Thruster pulse width	0.1 s
M_D	Thruster torque level	0.20 ft-lb
α	Thruster offset angle	45 deg
ϕ_c	Roll command	0.0286 deg
t_c	Roll command duration	70 s
t_I	Inhibit duration	430 s

Momentum Resolution

The three wheels comprise a redundant set with only two of them in operation at any particular time. Control loops are used to vary the wheel speed such that pitch is controlled by varying the Y-axis momentum about $-H_N$, and roll is controlled by varying the Z-axis momentum about zero. The control loops are configured to command Y- and Z-axes angular momentum components independently of which two of the three wheels are operating. Hence, momentum command distribution matrices are used to convert the Y- and Z-axes angular momentum commands (H_{YC} and H_{ZC}) to wheel momentum commands (H_{1C}, H_{2C}, and H_{3C}). The momentum command distribution matrices are:

1) Yaw wheel and negative cant pitch wheel operating

$$\begin{bmatrix} H_{1C} \\ H_{2C} \\ H_{3C} \end{bmatrix} = \begin{bmatrix} 0 & 0 \\ 1/\cos\beta & 0 \\ \tan\beta & 1 \end{bmatrix} \begin{bmatrix} H_{YC} \\ H_{ZC} \end{bmatrix} \tag{15}$$

2) Yaw wheel and positive cant pitch wheel operating

$$\begin{bmatrix} H_{1C} \\ H_{2C} \\ H_{3C} \end{bmatrix} = \begin{bmatrix} 1/\cos\beta & 0 \\ 0 & 0 \\ -\tan\beta & 1 \end{bmatrix} \begin{bmatrix} H_{YC} \\ H_{ZC} \end{bmatrix} \tag{16}$$

3) Positive cant and negative cant pitch wheels operating

$$\begin{bmatrix} H_{1C} \\ H_{2C} \\ H_{3C} \end{bmatrix} = \begin{bmatrix} \frac{1}{2\cos\beta} & \frac{1}{2\sin\beta} \\ \frac{1}{2\cos\beta} & \frac{-1}{2\sin\beta} \\ 0 & 0 \end{bmatrix} \begin{bmatrix} H_{YC} \\ H_{ZC} \end{bmatrix} \tag{17}$$

Similarly, the angular momentum of each wheel, as measured by its tachometer (H_{1M}, H_{2M}, and H_{3M}), must be resolved in the body frame (H_{YM} and H_{ZM}) to be of use to the control loops. The momentum measurement distribution matrix is

$$\begin{bmatrix} H_{YM} \\ H_{ZM} \end{bmatrix} = \begin{bmatrix} \cos\beta & \cos\beta & 0 \\ \sin\beta & -\sin\beta & 1 \end{bmatrix} \begin{bmatrix} H_{1M} \\ H_{2M} \\ H_{3M} \end{bmatrix} \tag{18}$$

Control System Tests

The control system tests utilized actual control system hardware operating in conjunction with an analog computer that simulated the spacecraft dynamics. The boresight axis of a dual scan horizon sensor was aligned with a heated Earth simulator target to generate sensor noise from the system tests. This noise was summed with the attitude signals from the computer-simulated dynamics to form simulated sensor inputs to the breadboard control electronics. Depending upon operating mode, the control electronics either drove simulated thrusters on the analog computer or bench-mounted reaction wheels. Torque transducers and tachometers were used to close the wheel control loops through the analog computer. The wheel configuration tested was with the yaw wheel and the negative cant pitch wheel operating. The parameter values used for the system are given in Table 2.

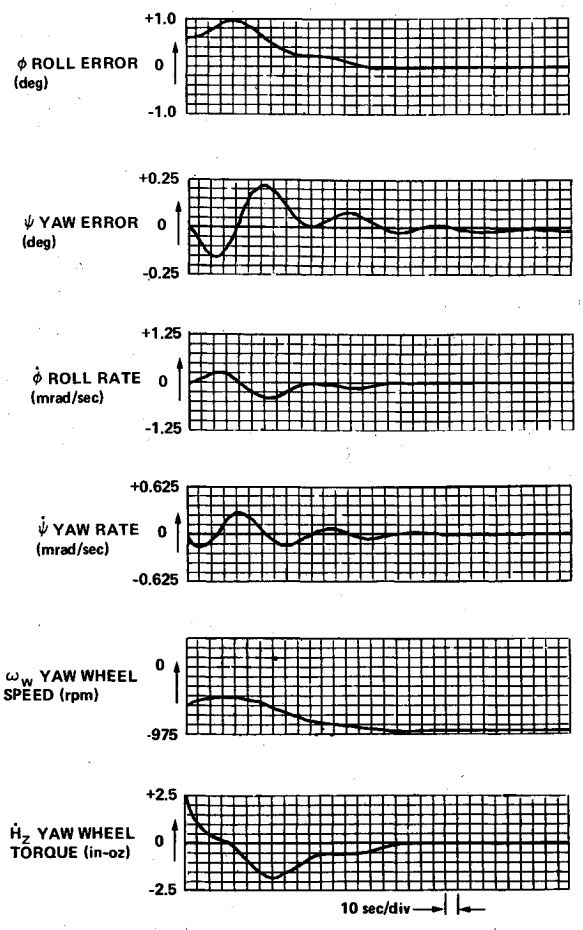

Fig. 7 Capture from an initial roll error of 0.6 deg.

Figure 7 shows the response to an initial roll offset of $\phi_0 = 0.6$ deg when the yaw wheel control loop is operating. This initial offset produces a Z_0 component of angular momentum of $-H_N \sin\phi_0$, assuming the pitch axis momentum bias is $-H_N$. This momentum must be transferred by the control loop to the yaw wheel in order to correct the roll error. Hence, the change in wheel speed is approximately given by

$$\Delta\omega_w = 1/6 \cdot H_N \phi_0 / I_w = 370.4 \text{ rpm} \tag{19}$$

assuming a small initial roll offset and ignoring orbit rate effects. This relationship gives the maximum roll error that the yaw wheel loop operating alone can capture from as

$$\phi_{0\max} = 6 I_w \Delta\omega_{w\max} / H_N = 0.89 \text{ deg} \tag{20}$$

These observations are based on momentum considerations alone and are independent of the form of the yaw wheel loop compensation electronics. The details of the transient response are dependent upon the form of the compensation network used. The Terasaki nonminimum phase zero compensation results in well-damped roll/yaw motion, but does produce some rather unusual short-term transient phenomena. For example, in correcting an initial roll error, the roll angle initially increases before decreasing. For parameter values chosen to give damping ratios and natural frequencies that satisfy the relationships[1]

$$\zeta_1 = 0.0175 \qquad \zeta_2 = 0.707 \qquad \zeta_1\omega_1 = \zeta_2\omega_2 \tag{21}$$

the maximum overshoot is approximately 1.55 ϕ_0 and occurs at two-thirds of a nutation period into the transient.

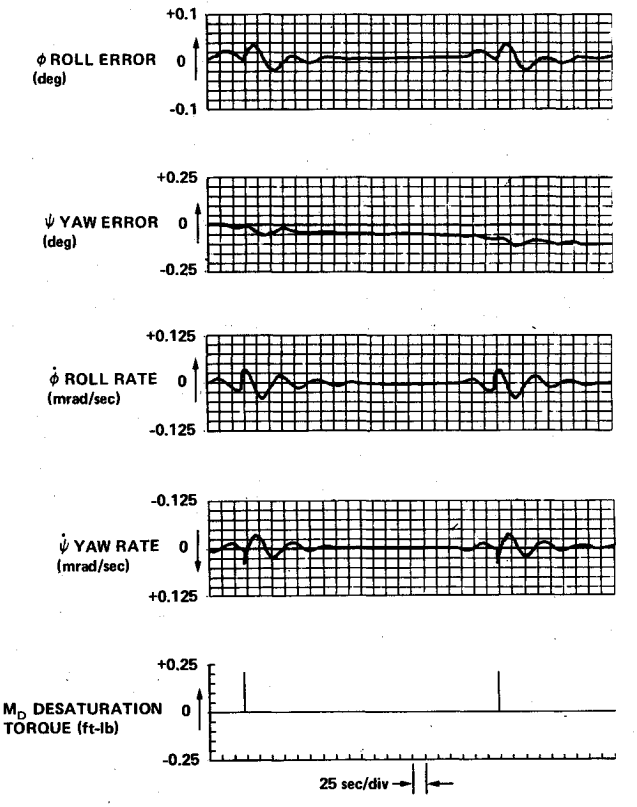

Fig. 8 Response to yaw axis momentum desaturation pulses.

Figure 8 shows the response of the yaw wheel control loop to the operation of the yaw wheel desaturation system. Body-fixed constant torques of $M_{BX} = 5 \times 10^{-5}$ ft-lb and $M_{BZ} = -5 \times 10^{-5}$ ft-lb were applied to the simulated vehicle dynamics in order to force the desaturation system into its deadband and produce two successive desaturation pulses. The output of the deadband circuit is the input to a pulse generator circuit that performs the following operations. First, a roll command or bias of $\phi_c = 0.0286$ deg is subtracted from the roll horizon sensor output for a period of $t_c = 70$ s. At the end of this period the roll command is removed and, simultaneously, a 100-ms pulse is delivered to the appropriate desaturation thruster. Once the pulse generator circuit has initiated a roll command, it is inhibited from initiating any further new commands for a period of $t_c + t_I = 500$ s. The roll angle command ϕ_c is one-half of the amplitude of the expected roll transient due to the desaturation thruster firing and, consequently, the total roll transient then ranges from $-\phi_c$ to $+\phi_c$ rather than from 0 to $+2\phi_c$. The thruster delay time t_c and the inhibit time t_I are chosen to provide the yaw wheel speed control loop adequate time to damp out the transient motion caused by the roll command and by the thruster pulse.

Conclusions

The main conclusions and results of this effort can be summarized as follows. First, a systematic design procedure has been established that permits the rational selection of bias momentum and desaturation deadbands for momentum bias systems given the desired pointing accuracy and disturbance torque environment. Second, the sensitivity of the design to variations in the magnitudes of the environmental torque components can be readily determined without extensive time-domain simulations. Third, two-axis momentum storage configurations employing three wheels are often better suited for high-accuracy long-life missions than single-axis momentum storage configurations employing two wheels. Finally, a complete attitude control system has been designed

by this procedure and hybrid tests using hardware components tied into an analog computer have been performed that verify the analysis and simulation of the system. The future evolution of this system will be based on the use of digital electronics to estimate the disturbance torques and to readjust the desaturation loop strategy accordingly.

References

[1] Dougherty, H.J., Lebsock, K.L., and Rodden, J.J., "Attitude Stabilization of Synchronous Communications Satellites Employing Narrow-Beam Antennas," *Journal of Spacecraft and Rockets*, Vol. 8, Aug. 1971, pp. 834-841.

[2] Iwens, R.P., Fleming, A.W., and Spector, V.A., "Precision Attitude Control with a Single Body Fixed Momentum Wheel," AIAA Paper 74-894, Anaheim, Calif., Aug. 1974.

[3] Terasaki, R.M., "Dual Reaction Wheel Control of Spacecraft Pointing," Symposium of Attitude Stabilization and Control of Dual Spin Spacecraft, SAMSO and Aerospace Corporation, El Segundo, Calif., Aug. 1967.

[4] Dahl, P.R., "A Twin Wheel Momentum Bias/Reaction Jet Spacecraft Control System," AIAA Paper 71-951, Hofstra University, Hempstead, N.Y., Aug. 1971.

[5] Dougherty, H.J., Scott, E.D., and Rodden, J.J., "Analysis and Design of Whecon—An Attitude Control Concept," AIAA Paper 68-461, San Francisco, Calif., April 1968.

[6] Collins, D.H. and Bonello, D.P., "An Attitude Control System for Earth Observation Spacecraft," AIAA Paper 73-854, Key Biscayne, Fla., Aug. 1973.